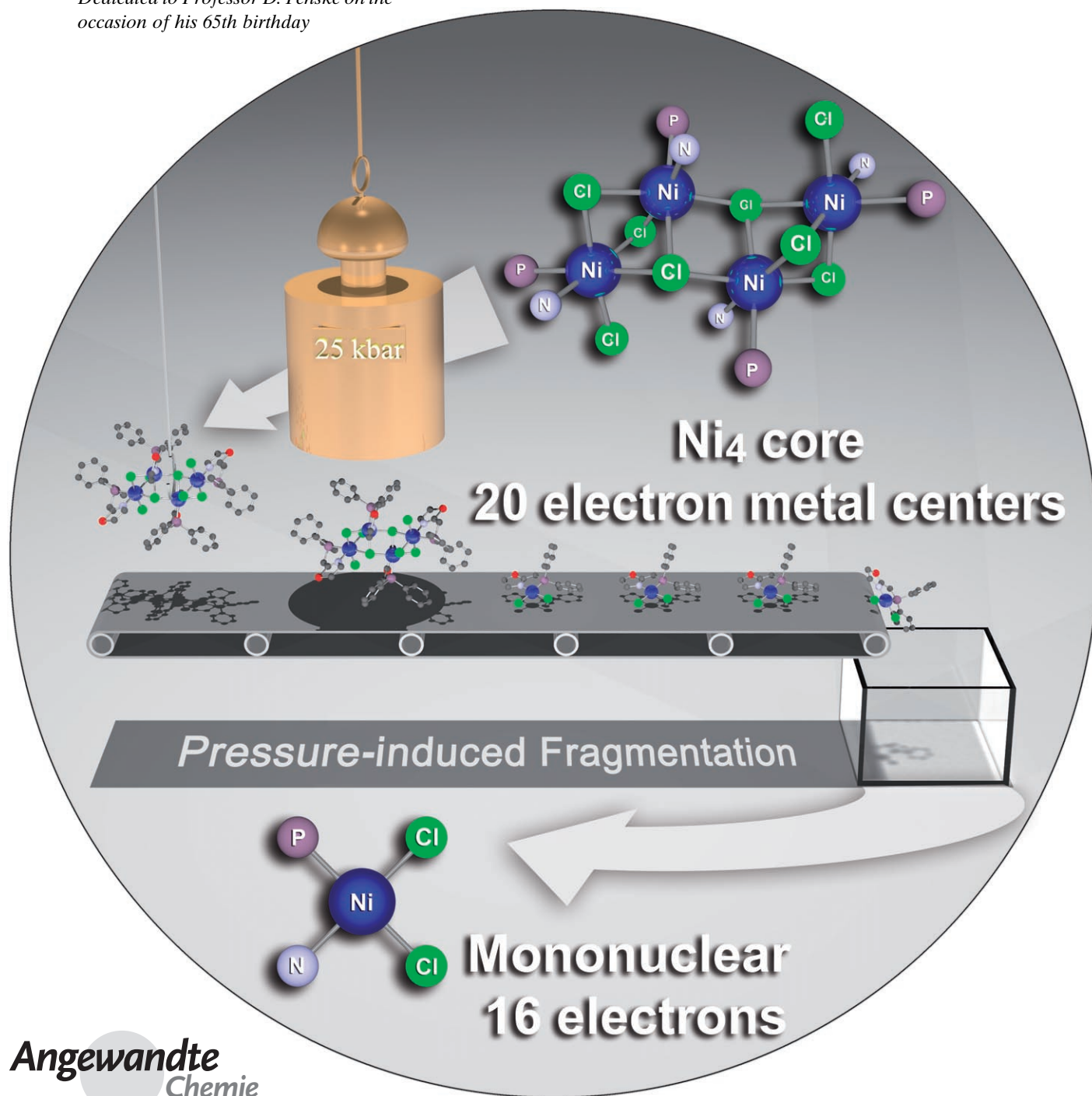


# Unprecedented Tetranuclear Complexes with 20-Electron $\text{Ni}^{\text{II}}$ Centers: The Role of Pressure and Temperature on Their Solid-State and Solution Fragmentation\*\*

Anthony Kermagoret, Roberto Pattacini, Patricia Chavez Vasquez, Guillaume Rogez, Richard Welter, and Pierre Braunstein\*

Dedicated to Professor D. Fenske on the occasion of his 65th birthday



Angewandte  
Chemie

Ligands with phosphorus and nitrogen or oxygen donor atoms allow fine-tuning of the structural properties and reactivity (stoichiometric and catalytic) of their metal complexes.<sup>[1]</sup> In particular, complexes bearing diversely substituted phosphinothiazolines have been studied for their dynamic behavior and catalytic activity in a number of reactions.<sup>[1c,2]</sup>

The unique reactivity of phosphinothiazolines<sup>[3]</sup> triggered a comparison between the ligands 2-diphenylphosphino-methyl-2-thiazoline (PN<sub>th</sub>) and 2-diphenylphosphinomethyl-2-oxazoline (PN<sub>ox</sub>). Their reaction in CH<sub>2</sub>Cl<sub>2</sub> with NiCl<sub>2</sub> afforded red solutions, which upon slow evaporation at 25 °C yielded red powders of [NiCl<sub>2</sub>(PN<sub>th</sub>)] (**1**) and [NiCl<sub>2</sub>(PN<sub>ox</sub>)] (**2**), respectively. However, rapid precipitation afforded green powders (see the Supporting Information), and green single crystals of [(NiCl<sub>2</sub>(PN<sub>th</sub>))<sub>4</sub>·2CH<sub>2</sub>Cl<sub>2</sub>] (**1a**·2CH<sub>2</sub>Cl<sub>2</sub>) were grown from a solution of **1** (Figure 1).

In the centrosymmetric, tetranuclear structure of **1a**, each metal center is in a slightly distorted octahedral environment defined by a chelating PN<sub>th</sub> ligand and four chlorine atoms: Cl1 is terminally bound to Ni1, but Ni1 and Ni2 are symmetrically bridged by Cl3 and Cl4, and Cl2 asymmetrically bridges three metal centers with the unusual electron count of 20. The Ni1...Ni2 distance of 3.0951(5) Å indicates the absence of strong metal–metal interactions.

The Ni<sub>4</sub>Cl<sub>8</sub> core of **1a** is unprecedented; no complex with a M<sub>4</sub>X<sub>8</sub> (X = halogen) stoichiometry appears to have been reported for Group 10 metals. Furthermore, its geometry is new for any combination of transition metals with halogens, and **1a** represents the first complex in which a phosphine is coordinated to a NiCl<sub>4</sub> moiety. Only one example of a phosphine bound to a NiX<sub>4</sub> fragment has been reported (X = Br).<sup>[5]</sup>

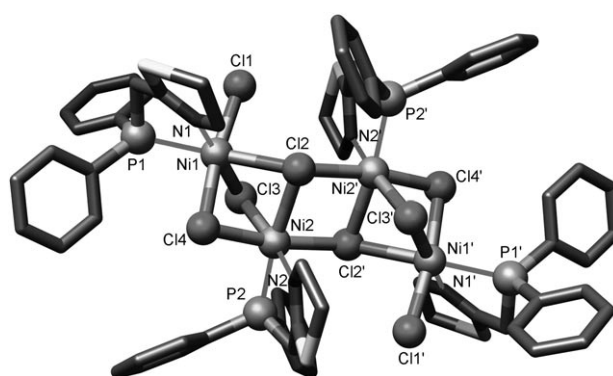
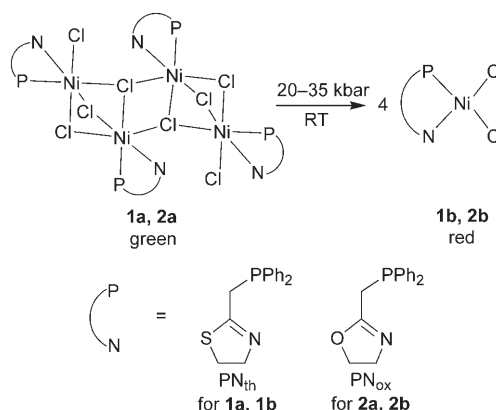


**Figure 1.** Molecular structure of **1a** in **1a**·2CH<sub>2</sub>Cl<sub>2</sub>. Hydrogen atoms omitted for clarity. Selected bond distances [Å] and angles [°]: Ni1...Ni2 3.0951(5), Ni1–Cl1 2.3357(7), Ni1–Cl2 2.6148(8), Ni1–Cl3 2.3870(8), Ni1–Cl4 2.4265(7), Ni2–Cl2 2.4534(8), Ni2–Cl2' 2.4307(8), Ni2–Cl3 2.4480(8), Ni2–Cl4 2.3972(8); Ni2–Cl2–Ni2' 93.79(3), Ni1–Cl2–Ni2' 134.50(3), Ni1–Cl2–Ni2 75.20(2), Ni1–Cl3–Ni2 79.59(3), Ni1–Cl4–Ni2 79.83(2). Symmetry operations generating equivalent atoms ('):  $-x, -y, -z$ .

The green complex [NiCl<sub>2</sub>(PN<sub>ox</sub>)]<sub>4</sub> (**2a**), analogous to **1a**, was obtained under similar conditions from PN<sub>ox</sub> and identified by X-ray powder diffraction (see the Supporting Information). In the solid state, complexes **1a** and **2a** undergo irreversible pressure-induced modification, with a color change from green to deep red (at 20–35 kbar; Scheme 1).



**Scheme 1.** Pressure-induced conversion of **1a** and **2a** into **1b** and **2b**, respectively.

Their high-pressure forms and the red powders obtained by slow solvent evaporation were identified as the mononuclear complexes [NiCl<sub>2</sub>(PN<sub>th</sub>)] (**1b**) and [NiCl<sub>2</sub>(PN<sub>ox</sub>)] (**2b**), respectively, by comparison of their FTIR spectra with those of the corresponding bromides **3** and **4** (Figure 2 and Figure S-1 in the Supporting Information).

The slightly distorted square-planar complexes **3** and **4** contain a PN chelate and two terminal bromides. The *trans* influence of the phosphorus donor makes the Ni1–Br2 bond longer than the Ni1–Br1 bond. Both PN ligands show analogous coordination geometries. The Ni–N and Ni–P bond lengths in **3** are much shorter than those observed in **1a**.

[\*] A. Kermagoret, Dr. R. Pattacini, P. Chavez Vasquez, Dr. P. Braunstein  
Laboratoire de Chimie de Coordination  
Institut de Chimie  
UMR 7177 CNRS  
Université Louis Pasteur  
4 rue Blaise Pascal, 67070 Strasbourg Cedex (France)  
Fax: (+33) 390-241-322  
E-mail: braunstein@chimie.u-strasbg.fr  
Homepage: <http://www-chimie.u-strasbg.fr/~lcc/>

Dr. G. Rogez  
Groupe des Matériaux Inorganiques  
IPCMS  
UMR 7504 CNRS  
23, rue du Loess, B.P. 43  
67034 Strasbourg Cedex 2 (France)

Prof. R. Welter  
DECOMET  
Institut de Chimie  
UMR 7177 CNRS  
Université Louis Pasteur  
4 rue Blaise Pascal, 67070 Strasbourg Cedex (France)

[\*\*] This work was supported by the Centre National de la Recherche Scientifique and the Ministère de l'Enseignement Supérieur et de la Recherche. We thank Dr. D. Mandon for assistance with the variable-temperature UV/Vis measurements.

Supporting information for this article is available on the WWW under <http://www.angewandte.org> or from the author.

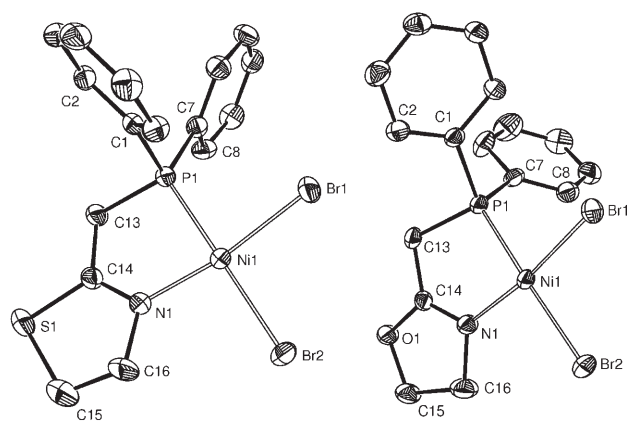


**Figure 2.** ORTEP views of the molecular structures of **3** (left) and **4** (right). Ellipsoids enclose 50% of the electron density. Hydrogen atoms omitted for clarity. Selected bond distances [Å] and angles [°]: **3**: Ni1–P1 2.147(1), Ni1–N1 1.910(3), Ni1–Br1 2.3095(6), Ni1–Br2 2.3665(6); N1–Ni1–P1 84.4(1), P1–Ni1–Br1 87.75(3), N1–Ni1–Br2 95.1(1), Br1–Ni1–Br2 92.72(2); **4**: Ni1–P1 2.158(1), Ni1–N1 1.905(3), Ni1–Br1 2.2983(7), Ni–Br2 2.3602(7), N1–Ni1–P1 85.0(1), P1–Ni1–Br1 87.73(4), N1–Ni1–Br2 94.0(1), Br1–Ni1–Br2 93.37(3).

The red solutions of **3** and **4** display magnetic moments of 1.3 and  $1.0\mu_{\text{B}}$ , respectively (Evans method<sup>[4]</sup>), which points to the presence of a paramagnetic isomer in equilibrium with the square-planar one (see below).

Relative to the FTIR spectrum of **2b** (Figure S-2 in the Supporting Information), that of **2a** displays split absorptions, which is consistent with two symmetry-independent ligands. In contrast to **1a** but similarly to **3** and **4**, one independent ligand is likely to be present in the unit cell of **1b**.

Few fully characterized pressure-induced isomerizations of nickel complexes have been reported: examples include the conversion from tetrahedral to dinuclear, square-pyramidal geometry,<sup>[6]</sup> and from mononuclear distorted tetrahedral to square-planar geometry.<sup>[7]</sup> A square-planar to octahedral isomerization was recently reported for a Pd thioether species.<sup>[8]</sup> Our system represents a more dramatic situation, involving: 1) the fragmentation of a tetranuclear complex with 20-electron metal centers into four 16-electron square-planar molecules and 2) an octahedral to square-planar rearrangement, associated with an overall density increase (estimated density from X-ray powder diffraction data for **2a**·2CH<sub>2</sub>Cl<sub>2</sub>: 1.41 and for **2b**, based on data for **4**: 1.55 g cm<sup>−3</sup>, see the Supporting Information).<sup>[9]</sup> The CH<sub>2</sub>Cl<sub>2</sub> molecules play a role in this phenomenon; their loss from the crystalline powders leaves voids that lower the density of the solid by approximately 10%, thus explaining the irreversibility of the process.

The magnetic properties of **2a** in the solid state were investigated in the range from 300 to 1.8 K with an applied field of 5 kOe. The Curie constant  $C = 4.64 \text{ emu K mol}^{-1}$ , determined from a fit of the  $1/\chi$  versus  $T$  curve to the Curie–Weiss law in the high-temperature region (150–300 K), is as expected for four octahedral Ni<sup>II</sup> ions ( $g = 2.15$ ).<sup>[10]</sup> The  $\chi T$  product decreases regularly upon cooling from  $4.54 \text{ emu K mol}^{-1}$  at 300 K to  $3.47 \text{ emu K mol}^{-1}$  at 20 K, indicating at least one intramolecular antiferromagnetic

interaction. Below 20 K, the small increase of the  $\chi T$  product up to  $3.49 \text{ emu K mol}^{-1}$  at 14 K and the final decrease below 14 K are probably due to a complicated interaction scheme and to competing intramolecular interactions (Figure 3 and

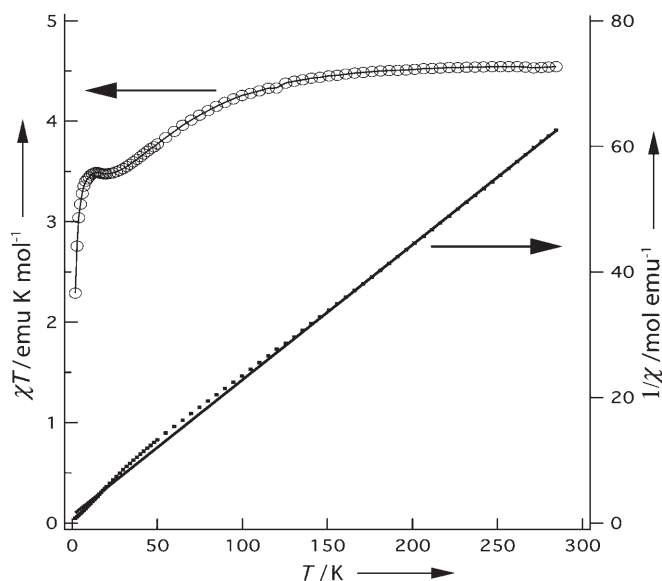


**Figure 3.**  $\chi T$  (○) and  $1/\chi$  (■) for **2a** as a function of temperature. Solid line: fit of the  $1/\chi$  versus  $T$  curve to the Curie–Weiss law in the region 150–300 K.

the Supporting Information) as well as to zero-field splitting. A paramagnetic impurity that obeys the Curie law ( $\chi = C/T$ ) would lead to a constant additive contribution in  $\chi T$ , which could not explain the slight increase of the  $\chi T$  product observed between 20 and 14 K. So far, no analytical fitting by full diagonalization of the complete spin Hamiltonian was successful over the whole temperature range. Further studies are in progress to determine the magnitude and sign of the different exchange constants and the characteristics of the ground state.

The red solutions of **1a/b** and **2a/b** change to green at low temperatures (Figure 4). A strong absorption band at 517 nm dominates the spectrum recorded at 293 K. Two weak bands centered at 615 and 700 nm were also detected. When the temperature was decreased, the main absorption band

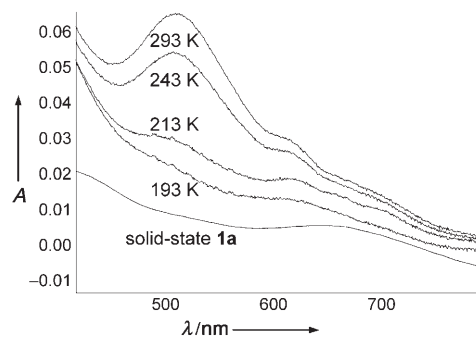


**Figure 4.** Visible spectra of **1a/b** in MeCN/CH<sub>2</sub>Cl<sub>2</sub> (5:2) in the range 293–193 K and of solid **1a** at room temperature.

disappeared and the two minor ones remained almost unchanged. The pattern of the spectrum at 193 K is similar to that of solid **1a**, suggesting that **1a** is present in solution and favored at low temperature, being enthalpically stabilized with respect to **1b**. The equilibrium was fully restored at 293 K.

The presence of two species in equilibrium in solution is consistent with the paramagnetism detected by the Evans method. The values of 2.8 and  $2.3\mu_B$  for **1** and **2**, respectively, in  $CD_2Cl_2$  are not consistent with either square-planar or octahedral coordination geometry. The paramagnetic NMR data for **1–4** could thus result from an equilibrium between a mononuclear diamagnetic complex and a polynuclear, probably tetranuclear, paramagnetic one. This equilibrium explains why rapid precipitation of a solution of **1b** or **2b** affords **1a** or **2a**, respectively, since precipitation shifts the equilibrium towards the less soluble species. Equilibria between square-planar and octahedral Ni complexes in solution are not uncommon and may involve solvation<sup>[11]</sup> and hemilability.<sup>[12]</sup> Other examples include tetrahedral to square-planar isomerism.<sup>[13]</sup> However, the present equilibrium between mononuclear and polynuclear Ni complexes with the same molecular formula appears unprecedented. The tetranuclear form is more stabilized in the case of  $PN_{th}$  than of  $PN_{ox}$ , as observed by 1) the Evans method and 2) the dependence of  $K$  on temperature.

The situations encountered in this work reveal many unprecedented features and indicate that subtle differences may result from the presence of oxygen or sulfur in  $PN_{ox}$  and  $PN_{th}$ , respectively.

### Experimental Section

Crystal data: **1a**:  $C_{64}H_{64}Cl_8Ni_4P_4S_4 \cdot 2CH_2Cl_2$ ,  $T = 193$  K,  $M = 1829.60$ , triclinic  $P\bar{1}$ ,  $a = 11.248(1)$ ,  $b = 11.518(1)$ ,  $c = 14.843(2)$  Å,  $\alpha = 91.811(3)$ ,  $\beta = 94.041(3)$ ,  $\gamma = 97.161(3)^\circ$ ,  $V = 1901.6(3)$  Å<sup>3</sup>,  $Z = 1$ ,  $\rho_{calcd} = 1.598$  g cm<sup>-3</sup>,  $\mu(MoK\alpha) = 1.63$  mm<sup>-1</sup>,  $F(000) = 932$ ,  $2\theta_{max} = 60^\circ$ ,  $R_1 = 0.0485$ ,  $wR_2 = 0.1107$ ,  $R(int) = 0.0369$  parameters = 420, 17720 reflections measured, 7468 ( $I > 2\sigma(I)$ ). **3**:  $C_{16}H_{16}NSPNiBr_2$ ,  $T = 193$  K,  $M = 503.86$ , triclinic  $P\bar{1}$ ,  $a = 8.6595(3)$ ,  $b = 8.6983(2)$ ,  $c = 12.9457(4)$  Å,  $\alpha = 91.476(1)$ ,  $\beta = 98.175(1)$ ,  $\gamma = 111.337(1)^\circ$ ,  $V = 895.86(5)$  Å<sup>3</sup>,  $Z = 2$ ,  $\rho_{calcd} = 1.868$  g cm<sup>-3</sup>,  $\mu(MoK\alpha) = 5.74$  mm<sup>-1</sup>,  $F(000) = 496$ ,  $2\theta_{max} = 57.4^\circ$ ,  $R_1 = 0.0438$ ,  $wR_2 = 0.0965$ ,  $R(int) = 0.0380$  parameters = 199, 6954 reflections measured, 3318 ( $I > 2\sigma(I)$ ). **4**:  $C_{16}H_{16}NOPNiBr_2$ ,  $T = 193$  K,  $M = 503.86$ , triclinic  $P\bar{1}$ ,  $a = 8.6330(3)$ ,  $b = 8.7360(3)$ ,  $c = 11.8890(4)$  Å,  $\alpha = 104.2010(17)$ ,  $\beta = 96.7060(17)$ ,  $\gamma = 96.3230(12)^\circ$ ,  $V = 854.28(5)$  Å<sup>3</sup>,  $Z = 2$ ,  $\rho_{calcd} = 1.896$  g cm<sup>-3</sup>,  $\mu(MoK\alpha) = 5.90$  mm<sup>-1</sup>,  $F(000) = 480$ ,  $2\theta_{max} = 58.2^\circ$ ,  $R_1 = 0.0464$ ,  $wR_2 = 0.1194$ ,  $R(int) = 0.0429$  parameters = 199, 6589 reflections measured, 2768 ( $I > 2\sigma(I)$ ). CCDC-641491 (**1a**), 641489 (**3**), and 641490 (**4**) contain the supplementary crystallographic data for this paper. These data can be obtained free of charge from The Cam-

bridge Crystallographic Data Centre via [www.ccdc.cam.ac.uk/data\\_request/cif](http://www.ccdc.cam.ac.uk/data_request/cif).

Received: April 5, 2007

Revised: June 7, 2007

Published online: July 16, 2007

**Keywords:** isomerization · magnetic properties · N,P ligands · nickel · polynuclear complexes

- [1] See, for example, a) P. Braunstein, *Chem. Rev.* **2006**, *106*, 134–159; b) P. Braunstein, F. Naud, *Angew. Chem.* **2001**, *113*, 702–722; *Angew. Chem. Int. Ed.* **2001**, *40*, 680–699; c) G. Helmchen, A. Pfaltz, *Acc. Chem. Res.* **2000**, *33*, 336–345; d) C. S. Slone, D. A. Weinberger, C. A. Mirkin, *Prog. Inorg. Chem.* **1999**, *48*, 233–250.
- [2] a) F. Speiser, P. Braunstein, L. Saussine, *Acc. Chem. Res.* **2005**, *38*, 784–793; b) P. Braunstein, G. Clerc, X. Morise, R. Welter, G. Mantovani, *Dalton Trans.* **2003**, 1601–1605; c) P. Braunstein, G. Clerc, X. Morise, *New J. Chem.* **2003**, *27*, 68–72; d) P. Braunstein, F. Naud, A. Dedieu, M.-M. Rohmer, A. DeCian, S. J. Rettig, *Organometallics* **2001**, *20*, 2966–2981; e) P. Braunstein, F. Naud, S. J. Rettig, *New J. Chem.* **2001**, *25*, 32–39; f) P. Braunstein, C. Graiff, F. Naud, A. Pfaltz, A. Tiripicchio, *Inorg. Chem.* **2000**, *39*, 4468–4475; g) P. Braunstein, M. D. Fryzuk, M. Le Dall, F. Naud, S. J. Rettig, F. Speiser, *J. Chem. Soc. Dalton Trans.* **2000**, 1067–1074; h) J. Sprinz, G. Helmchen, *Tetrahedron Lett.* **1993**, *34*, 1769–1772.
- [3] G. Margraf, R. Pattacini, A. Messaoudi, P. Braunstein, *Chem. Commun.* **2006**, 3098–3100.
- [4] a) D. F. Evans, *J. Chem. Soc. A* **1959**, 2003–2005; b) S. K. Sur, *J. Magn. Reson.* **1989**, *82*, 169–173.
- [5] P. B. Hitchcock, T. H. Lee, G. J. Leigh, *Dalton Trans.* **2003**, 2276–2279.
- [6] G. J. Long, J. R. Ferraro, *J. Chem. Soc. Chem. Commun.* **1973**, 719–720.
- [7] J. R. Ferraro, K. Nakamoto, J. T. Wang, L. Lauer, *J. Chem. Soc. Chem. Commun.* **1973**, 266–267.
- [8] D. R. Allan, A. J. Blake, D. Huang, T. J. Prior, M. Schröder, *Chem. Commun.* **2006**, 4081–4083.
- [9] For a recent review on high-pressure chemistry, see: W. Grochala, R. Hoffmann, J. Feng, N. W. Ashcroft, *Angew. Chem.* **2007**, *119*, 3694–3717; *Angew. Chem. Int. Ed.* **2007**, *46*, 3620–3642.
- [10] R. L. Carlin, *Magneto-chemistry*, Springer, Berlin, **1986**.
- [11] S. Mukhopadhyay, D. Mandal, D. Ghosh, I. Goldberg, M. Chaudhury, *Inorg. Chem.* **2003**, *42*, 8439–8445.
- [12] a) L. Sacconi, P. Nannelli, N. Nardi, U. Campigli, *Inorg. Chem.* **1965**, *4*, 943–949; b) L. Sacconi, N. Nardi, F. Zanobini, *Inorg. Chem.* **1966**, *5*, 1872–1876.
- [13] a) R. G. Hayter, F. S. Humiec, *J. Am. Chem. Soc.* **1962**, *84*, 2004–2005; b) R. G. Hayter, F. S. Humiec, *Inorg. Chem.* **1965**, *4*, 1701–1706.